MEMORANDUM REPORT BRL-MR-3436

COMPUTATIONAL MODELING OF THE BASE REGION FLOW FOR A PROJECTILE WITH A BASE CAVITY

Jubaraj Sahu
Charles J. Nietubicz

April 1985

US ARMY BALLISTIC RESEARCH LABORATORY
ABERDEEN PROVING GROUND, MARYLAND

Destroy this report when it is no longer needed.
Do not return it to the originator.

Additional copies of this report may be obtained from the National Technical Information Service, U. S. Department of Commerce, Springfield, Virginia 22161.

The findings in this report are not to be construed as an official Department of the Army position, unless so designated by other authorized documents.

The use of trade names or manufacturers' names in this report does not constitute indorsement of any commercial product.

UNCLASSIFIED

SECURITY CLASSIFICATION OF THIS PAGE *(When Date Entered)*

REPORT DOCUMENTATION PAGE

READ INSTRUCTIONS BEFORE COMPLETING FORM

1. REPORT NUMBER: MEMORANDUM REPORT BRL-MR-3436	2. GOVT ACCESSION NO.
3. RECIPIENT'S CATALOG NUMBER	
4. TITLE *(and Subtitle)*: COMPUTATIONAL MODELING OF THE BASE REGION FLOW FOR A PROJECTILE WITH A BASE CAVITY	5. TYPE OF REPORT & PERIOD COVERED
	6. PERFORMING ORG. REPORT NUMBER
7. AUTHOR(s): Jubaraj Sahu and Charles J. Nietubicz	8. CONTRACT OR GRANT NUMBER(s)
9. PERFORMING ORGANIZATION NAME AND ADDRESS: US Army Ballistic Research Laboratory ATTN: AMXBR-LFD Aberdeen Proving Ground, Maryland 21005-5066	10. PROGRAM ELEMENT, PROJECT, TASK AREA & WORK UNIT NUMBERS: RDT&E 1X464603D385
11. CONTROLLING OFFICE NAME AND ADDRESS: US Army Ballistic Research Laboratory ATTN: AMXBR-OD-ST Aberdeen Proving Ground, Maryland 21005-5066	12. REPORT DATE: April 1985 13. NUMBER OF PAGES: 33
14. MONITORING AGENCY NAME & ADDRESS *(if different from Controlling Office)*	15. SECURITY CLASS. *(of this report)*: Unclassified 15a. DECLASSIFICATION/DOWNGRADING SCHEDULE

16. DISTRIBUTION STATEMENT *(of this Report)*

Approved for public release; distribution unlimited.

17. DISTRIBUTION STATEMENT *(of the abstract entered in Block 20, if different from Report)*

18. SUPPLEMENTARY NOTES

This report supersedes BRL IMR No. 813 dated May 1984

19. KEY WORDS *(Continue on reverse side if necessary and identify by block number)*

Numerical Computations
Base Cavity
Axisymmetric Projectile
Time Dependent
Base Flow
Compressible Flow
Implicit Algorithm

20. ABSTRACT *(Continue on reverse side if necessary and identify by block number)*

Recent firing test results indicated some differences in drag between projectiles with modified base configurations. This report documents a computational study to predict the drag of shell with modified base configurations similar to the ones tested. Flow field computations using a thin layer Navier-Stokes computational technique have been performed for a PXR projectile configuration with and without a base cavity at M = .9 and α = 0. Computed results show the qualitative effect of the base cavity on the base region flow field.

(continued)

DD FORM 1 JAN 73 1473 EDITION OF 1 NOV 65 IS OBSOLETE

UNCLASSIFIED

SECURITY CLASSIFICATION OF THIS PAGE *(When Date Entered)*

20. ABSTRACT (Continued)

Quantitatively, a reduction in base drag of about 25% was found due to the cavity. The magnitude of this reduction may have been over predicted; also some questions as to whether or not the base region flow field is unsteady still remain to be investigated.

TABLE OF CONTENTS

LIST OF ILLUSTRATIONS

I. INTRODUCTION

Firing tests[1] of the PXR projectiles with modified base geometries have recently been performed. Analysis of the test results revealed small, but experimentally significant, differences in the observed effective drag. Therefore, it was desired to numerically compute the flow field for these configurations and determine the effect of the modified base geometries on the base region flow. The total drag for projectiles can be divided into three components: (i) pressure drag (excluding the base region), (ii) viscous or skin friction drag, and (iii) base drag. At transonic speeds the base drag constitutes a major portion of the total drag. Thus, the determination of base pressure for projectile configurations is essential in predicting the total drag coefficient.

A series of computations have recently been performed for a PXR projectile configuration in which the full range of aerodynamic coefficients have been determined.[2] The actual PXR configuration is a rocket assisted projectile and contains a base cavity as part of the base configuration. The previous computations[2] however, did not include the cavity and modeled the base as a solid wall. In pursuing the capability to compute the flow field of the actual projectile, a new capability has been developed which allows the base to include an annular cavity. Other base configurations which contain cylindrical cavities have not been considered in the present analysis. However, with minor modifications the developed code could handle such cavities. This report discusses the development of this capability and the preliminary results which have been obtained.

II. COMPUTATIONAL TECHNIQUE

The Azimuthal Invariant (or Generalized Axisymmetric) thin-layer Navier-Stokes equations for general spatial coordinates ξ, η, ζ can be written as[3]

$$\partial_\tau \hat{q} + \partial_\xi \hat{E} + \partial_\zeta \hat{G} + \hat{H} = Re^{-1} \partial_\zeta \hat{S} \qquad (1)$$

---

1. *Private Communications with Mr. Richard Eitemiller of the Firing Tables Branch, Launch and Flight Division, BRL, June 1983.*

2. *C. J. Nietubicz, R. LaFarge, J. Sahu, and D. C. Mylin, "Aerodynamic Coefficient Predictions for a Projectile Configuration at Transonic Speeds," AIAA Paper No. 84-0326, January 1984.*

3. *C. J. Nietubicz, T. H. Pulliam, and J. L. Steger, "Numerical Solution of the Azimuthal-Invariant Thin-Layer Navier-Stokes Equations," U.S. Army Ballistic Research Laboratory, Aberdeen Proving Ground, Maryland, ARBRL-TR-02227, March 1980. (AD A085716) (Also see AIAA Paper No. 79-0010, January 1979.*

where $\xi = \xi(x,y,z,t)$ is the longitudinal coordinate

$\eta = \eta(y,z,t)$ is the circumferential coordinate

$\zeta = \zeta(x,y,z,t)$ is the normal coordinate

$\tau = t$ is the time

and

$$\hat{q} = J^{-1}\begin{bmatrix} \rho \\ \rho u \\ \rho v \\ \rho w \\ e \end{bmatrix}, \quad \hat{E} = J^{-1}\begin{bmatrix} \rho U \\ \rho uU+\xi_x p \\ \rho vU+\xi_y p \\ \rho wU+\xi_z p \\ (e+p)U-\xi_t p \end{bmatrix}, \quad \hat{G} = J^{-1}\begin{bmatrix} \rho W \\ \rho uW+\zeta_x p \\ \rho vW+\zeta_y p \\ \rho wW+\zeta_z p \\ (e+p)W-\zeta_t p \end{bmatrix},$$

$$\hat{H} = J^{-1}\begin{bmatrix} 0 \\ 0 \\ \rho V[R_\xi(U-\xi_t) + R_\zeta(W-\zeta_t)] \\ -\rho VR\phi_\eta(V-\eta_t) - p/(R\phi_\eta) \\ 0 \end{bmatrix}$$

$$\hat{S} = \begin{bmatrix} 0 \\ \mu(\zeta_x^2 + \zeta_y^2 + \zeta_z^2)u_\zeta + (\mu/3)(\zeta_x u_\zeta + \zeta_y v_\zeta + \zeta_z w_\zeta)\zeta_x \\ \mu(\zeta_x^2 + \zeta_y^2 + \zeta_z^2)v_\zeta + (\mu/3)(\zeta_x u_\zeta + \zeta_y v_\zeta + \zeta_z w_\zeta)\zeta_y \\ \mu(\zeta_x^2 + \zeta_y^2 + \zeta_z^2)w_\zeta + (\mu/3)(\zeta_x u_\zeta + \zeta_y v_\zeta + \zeta_z w_\zeta)\zeta_z \\ \{(\zeta_x^2 + \zeta_y^2 + \zeta_z^2)[(\mu/2)(u^2 + v^2 + w^2)_\zeta + \kappa Pr^{-1}(\gamma - 1)^{-1}(a^2)_\zeta] \\ \quad + (\mu/3)(\zeta_x u + \zeta_y v + \zeta_z w)(\zeta_x u_\zeta + \zeta_y v_\zeta + \zeta_z w_\zeta)\} \end{bmatrix}$$

The velocities

$$U = \xi_t + \xi_x u + \xi_y v + \xi_z w$$

$$V = \eta_t + \eta_x u + \eta_y v + \eta_z w$$

$$W = \zeta_t + \zeta_x u + \zeta_y v + \zeta_z w$$

represent the contravariant velocity components. Equation (1) is solved in a time asymptotic fashion with interest only in the steady-state solution. The numerical algorithm used is a fully implicit, approximately factored finite difference scheme. The algorithm is first order accurate in time and fourth order in space. A two-layer algebraic eddy viscosity model[4] is included for the computation of turbulent flows. Details of the assumptions and the algorithm are included in References 5-7.

III. METHOD OF SOLUTION

A. Base Region Flow without Cavity

The procedure used to compute the base flow for shell without the base cavity has been described in Reference 8; however, limited details are repeated here for clarity. The base flow code computes the full flow field (including the base region) of a projectile. Figure 1 shows a schematic illustration of the flow field segmentation and shows the transformation of the physical domain into the computational domain. This flow field segmentation procedure is equivalent to using multiple adjoining grids. An important advantage of this procedure lies in the preservation of the sharp corner at the base and allows easy blending of the computational meshes between the regions ABCD and AEFG. No approximation of the actual sharp corner at the base is made. Thus, realistic representation of the base is inherent in the current procedure.

The cross hatched region in the physical domain represents the model. The line BC is the base and the region ABCD is the base region or the wake. The line AB is a computational cut through the physical wake region which acts as a repetitive boundary in the computational domain. Implicit integration is carried out in both ξ and ζ directions (see Figure 1). Note the presence of

---

4. *B. S. Baldwin, and H. Lomax, "Thin-Layer Approximation and Algebraic Model for Separated Turbulent Flows," AIAA Paper No. 78-257, 1978.*

5. *R. Beam, and R. F. Warming, "An Implicit Factored Scheme for the Compressible Navier-Stokes Equations," AIAA Journal, Vol. 16, No. 4, April 1978, pp. 393-402.*

6. *J. L. Steger, "Implicit Finite Difference Simulation of Flow About Arbitrary Geometries with Application to Airfoils," AIAA Journal, Vol. 16, No. 4, July 1978, pp. 679-686.*

7. *T. H. Pulliam, and J. L. Steger, "On Implicit Finite-Difference Simulations of Three-Dimensional Flow," AIAA Journal, Vol. 18, No. 2, February 1980, pp. 159-167.*

8. *J. Sahu, C. J. Nietubicz, and J. L. Steger, "Numerical Computation of Base Flow for a Projectile at Transonic Speeds," U.S. Army Ballistic Research Laboratory, Aberdeen Proving Ground, Maryland, ARBRL-TR-02495, June 1983. (AD A130293) (Also see AIAA Paper No. 82-1358, August 1982).*

the lines BC (base) and EF (nose axis) in the computational domain. They both act as boundaries in the computational domain and special care must be taken in inverting the block tridiagonal matrix in the ξ direction. The details of these can be found in References 8 and 9 and are not included here.

The no slip boundary condition for viscous flow is enforced by setting

$$U = V = W = 0 \tag{2}$$

on the body surface. At the base boundary, an inviscid boundary condition has been used. Additionally, at the corner of the base, the boundary conditions are double-valued and depend on the direction from which the corner is approached. Approaching the corner in the streamwise direction (EB), the no-slip boundary condition is used while approaching in the radial direction (along the base, CB), the inviscid boundary condition is used. Along the computational cut (AB), the flow variables above and below the cut are simply averaged to determine the boundary conditions on the cut. On the centerline of the wake region, a symmetry condition is imposed and free stream conditions are used on the outer boundary.

B. Base Region Flow with Cavity

The procedure used to compute the base flow including the effect of the cavity is now described. The flow field segmentation procedure described above takes a new form shown schematically in Figure 2. There are two flow field regions AEFG and ABPRSQCD. The latter one contains the base cavity PRSQ. The two cross hatched regions in the computational domain are the aft end of the projectile and computations are not made in these regions. The presence of such rectangular regions inside the computational domain requires special care in carrying out the integrations both in the ξ and the ζ directions. Modeling the base cavity in this manner requires specification of boundary conditions on the new boundaries PR, RS and SQ and special monitoring of the ξ and ζ indices.

The boundary conditions on the body surface, the cut and the downstream boundary remain the same as described earlier. Along the base (lines BP, QC and RS) inviscid boundary conditions are used. Inviscid boundary conditions are also used for lines PR and SQ. The turbulence model has not been modified for this region and the same length scales used for the near wake are used in the cavity.

---

9. *J. Sahu, C. J. Nietubicz, and J. L. Steger, "Navier-Stokes Computations of Projectile Base Flow with and without Base Injection," U.S. Army Ballistic Research Laboratory, Aberdeen Proving Ground, Maryland, ARBRL-TR-02532, November 1983. (AD A135783) (Also see AIAA Paper No. 83-0224, January 1983).*

IV. MODEL AND GRID

The basic model geometry used in this study, excluding the details of the base is shown in Figure 3. It is a secant-ogive-cylinder-boattail configuration. The base region configurations of interest are shown in Figure 4. These configurations all contain annular cavities. Free flight tests have previously been conducted on a SAMOS re-entry configuration[10] which contained a cylindrical cavity. Cylindrical cavities are not included in the present analysis. In this report, the annular base cavity shown in Figure 4(a) has been modeled.

The computational grid used for the numerical calculations was obtained from a grid generator described in Reference 11. This program allows arbitrary grid point clustering, thus enabling grid points for the projectiles to be clustered in the vicinity of the body surface. The full grid is shown in Figure 5 while Figure 6 shows an expanded view of the grid near the model. The grid consists of 114 points in the longitudinal direction and 40 points in the normal direction. For the base region, 30 grid points were used in the streamwise direction. The grid nodes in the normal direction are clustered near the surface to capture viscous effects. These points were exponentially stretched away from the surface with a minimum spacing of .00002D at the wall. This locates at least two points in the laminar sublayer. As can be seen in Figure 6, the grid points in the longitudinal direction are clustered near the cylinder and boattail junctions and also at the base where large gradients in flow variables are expected to occur.

An expanded view of the grid in the base region for the case of a solid base is shown in Figure 7. Figure 8 shows the grid in the base region including the cavity. For computations of base flow with base cavity it is necessary to locate an adequate number of grid points in the cavity region and the exponential stretching used previously is not suitable. Therefore, a 1-D elliptic solver was used to obtain the grid spacings in the normal direction ζ for the base region with the cavity. In both cases with and without the cavity, the minimum spacing on both sides of the cut (AB) was the same (.00002D). Thus, a smooth variation of the grid is maintained across the cut.

V. RESULTS

Computations for the PXR projectile, both with and without the cavity, have been made at $M = 0.9$ and $\alpha = 0$. Both qualitative and quantitative results are now presented for these base configurations. Figure 9 shows the

---

10. *E. D. Boyer, "Free Flight Tests of the SAMOS Re-entry Configuration," U.S. Army Ballistic Research Laboratory, Maryland, ARBRL-MR-1321, February 1961. (AD 374655L)*

11. *J. L. Steger, C. J. Nietubicz, and K. R. Heavey, "A General Curvilinear Grid Generation Program for Projectile Configurations," U.S. Army Ballistic Research Laboratory, Maryland, ARBRL-MR-03142, October 1981. (AD A107334)*

velocity vectors in the base region for the case with no cavity. The recirculatory flow in the near wake is clearly evident. The reattachment point is less than a caliber downstream of the base. The effect of the cavity on the base region flow field is shown in Figure 10. The base region flow field is now characterized by two recirculation regions of opposite sign. A small bubble is formed inside the cavity which has displaced the shear layer. The recirculation bubble in the near wake is now larger and the reattachment point has been moved further downstream to a position 1.5 calibers from the base.

A more critical look at the computational results is presented in Figures 11 and 12. Recall that the computational technique used in these calculations is a time dependent, implicit algorithm and the unsteady set of equations are marched in time to obtain the steady state results. An implicit algorithm, in general, allows large time steps in order to reach the desired steady state solution. However, large time steps can often give rise to numerical oscillations as evidenced by results shown in Figures 11 and 12. Figure 11 and 12 show the variation of base drag and total drag respectively with time. With a non-dimensional time, $\Delta\tau = .01$, the solutions indicate an unsteady flow field. The time step was reduced to .005 and the amplitude of the oscillations dropped. The amplitude of the oscillations was further reduced for a time step of .0025. This indicates that the flow field in the base region with the cavity may not be unsteady. However, it requires a different approach for advancing in time to get the desired steady state results. This type of oscillation was not found in the computations of the base flow without the cavity.

Such oscillations are believed to be numerical rather than physical and are dependent on the flow problem. Similar oscillations were also observed in a time dependent numerical computation[12] of supersonic flow over a ramp. Additionally, these oscillations were not observed when the eddy viscosity turbulence model was frozen.[12] This again suggests that the oscillations in the present calculations are not physical and are probably due to the interaction of the turbulence model with the flow field.

The total drag as shown in Figure 12 is converging to a lower value with the cavity as compared to the corresponding value of total drag obtained for the solid base. Other drag components such as pressure drag and skin friction drag remained practically the same both with or without the cavity. The influence of the cavity on the flow field upstream of the base corner is negligible. Thus, no significant change in pressure drag or skin friction drag was found. The cavity, however, has a large influence on the flow field in the base region, especially in the near wake. Thus, the base drag is strongly affected. Any change in the base drag is, of course, reflected in the total aerodynamic drag.

As can be seen from Figure 12, a reduction in the total drag due to the cavity of about 25% is predicted. The effect of a base region cavity on the

---

12. *D. Degani, and J. L. Steger, "Comparison Between Navier-Stokes and Thin-Layer Computations for Separated Supersonic Flow,"* AIAA Journal, *Vol. 21, No. 11, November 1983, pp. 1604-1606.*

base pressure has been studied by other researchers.[13] The trend in the reduction of base drag as a function of Mach number is shown in Figure 13 and is reproduced from Reference 13. As shown in Figure 13, reduction in base drag due to a cavity of about 20% was observed at subsonic and transonic speeds. Whether or not the base pressure is affected by the presence of a cavity in supersonic flow is not clear. The present computed results show a reduction in drag of about 25% at M = .9. The effect of the base cavity on the base flow has thus been correctly predicted qualitatively. Direct quantitative comparison of the magnitude of the drag reduction has not been made since such data is not available. These results are considered to be preliminary and further computational effort is required.

VI. CONCLUDING REMARKS

A computational predictive capability has been developed to compute the base flow for shell with a base cavity. Numerical computations have been made for the PXR projectile both with and without the cavity at M = .9 and α = 0.

Flowfield results, both with and without the cavity have been presented. The presence of the cavity has been shown to have a large influence on the near wake flow field. A small recirculation bubble is formed inside the cavity which displaces the shear layer and forces the rear stagnation point further downstream of the base.

Quantitatively, the cavity has practically no effect on the pressure drag and the skin friction drag but strongly affects the base drag. A reduction in base drag and thus the total drag of about 25% has been found due to the base cavity. The magnitude of this reduction may be overpredicted due to grid resolution and/or the turbulence model. Additionally, oscillations in the computed solutions were observed which are believed to be numerical rather than physical. These oscillations seem to die out when smaller and smaller time steps are taken and solutions are marched in time to obtain the desired steady state results. Some questions as to whether the flow field in the base region is unsteady or not still remain. Future computations must address these issues.

---

13. *S. N. B. Murthy (Ed.), "Progress in Astronautics and Aeronautics: Aerodynamics of Base Combustion," Vol. 40, AIAA, New York, 1976, pp. 90-92.*

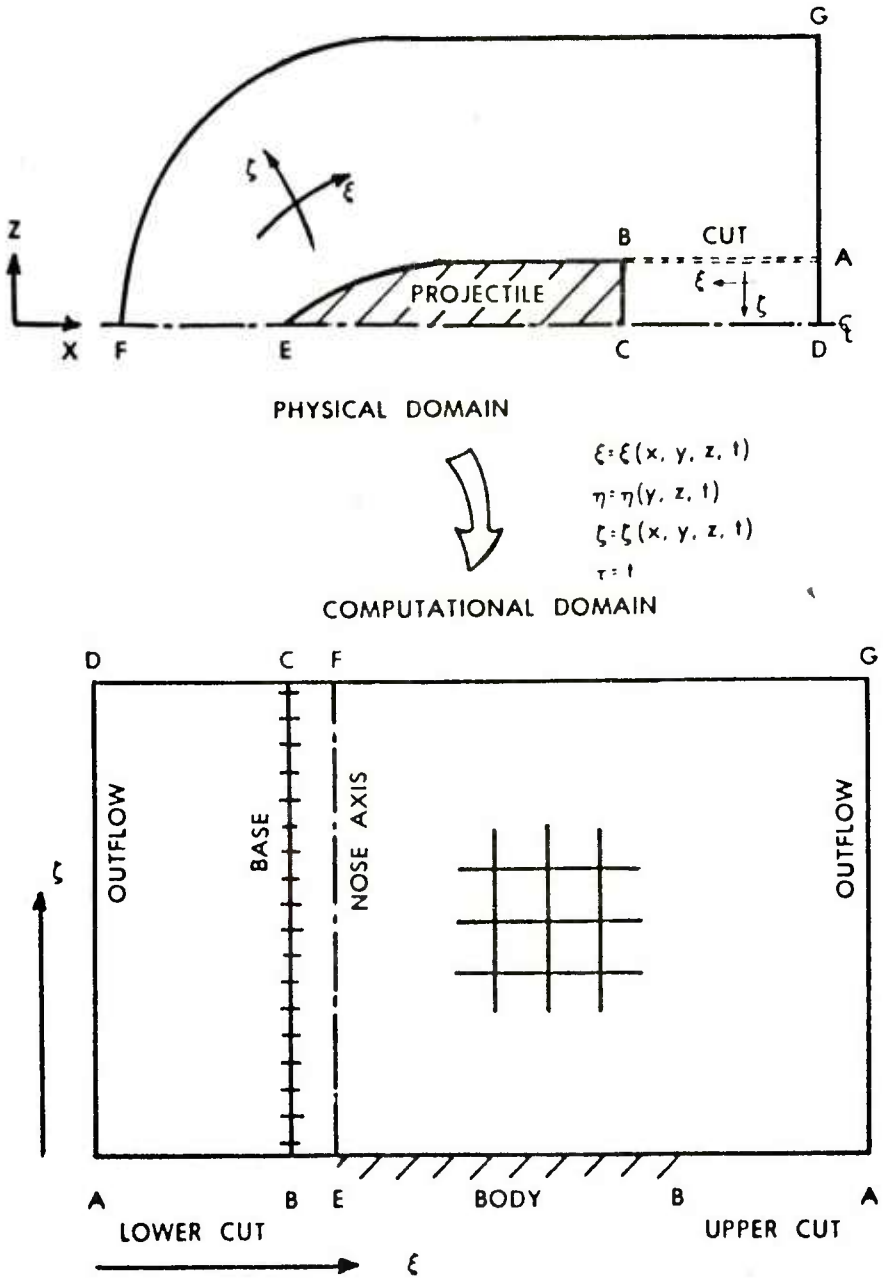

Figure 1. Flow Field Segmentation (without base cavity)

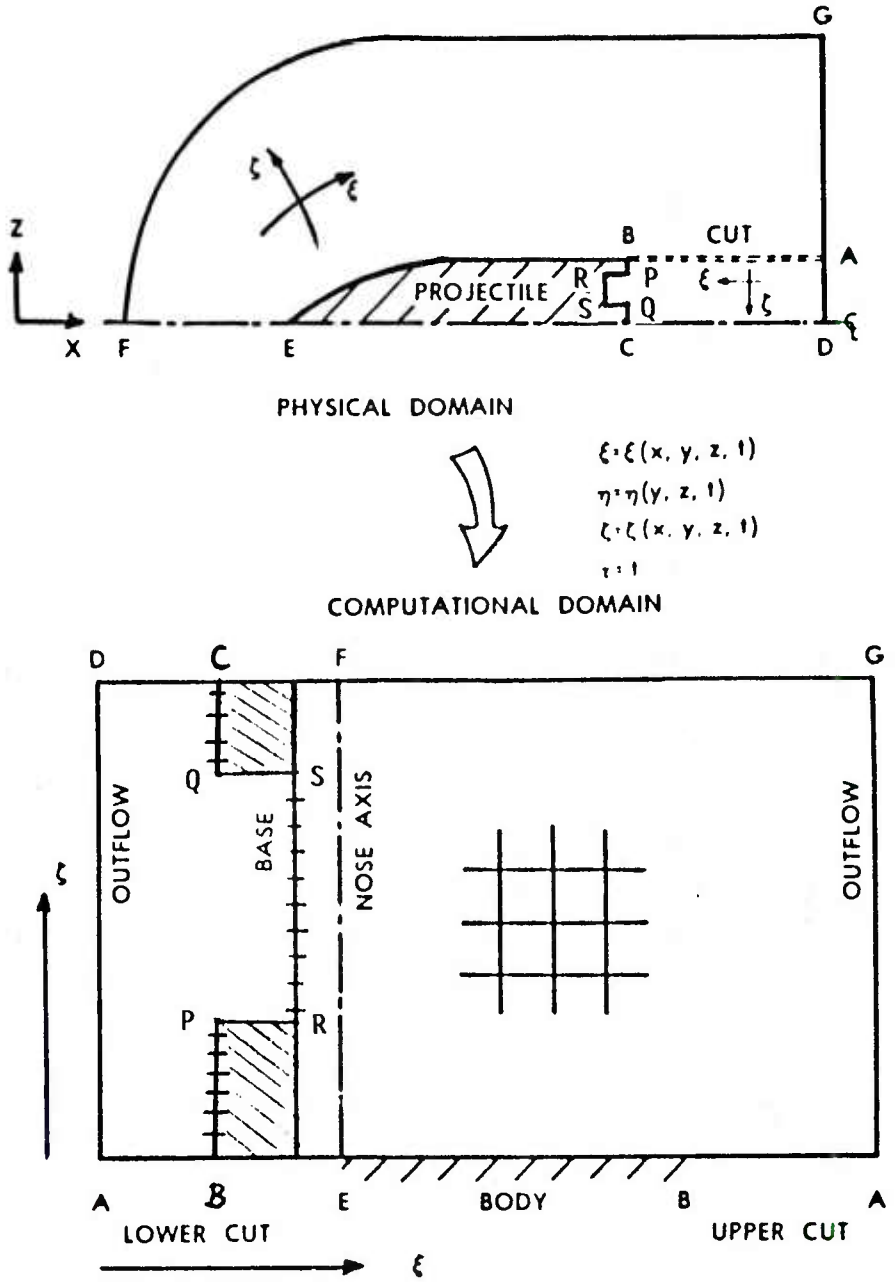

Figure 2. Flow Field Segmentation (with base cavity)

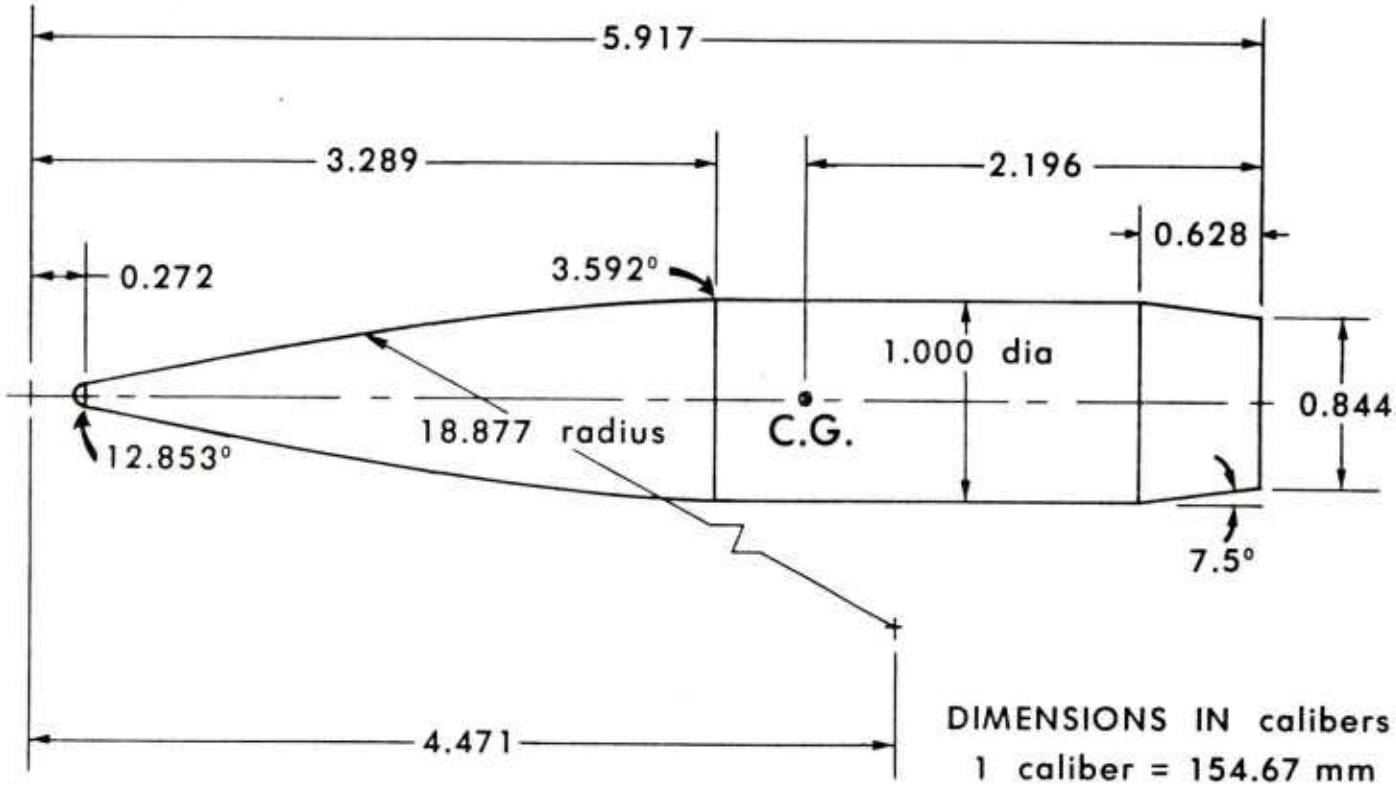

Figure 3. Model Geometry

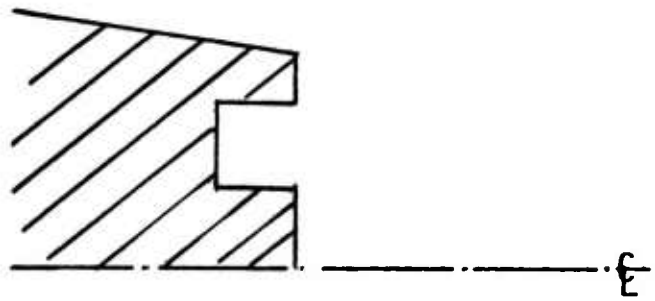

(A)

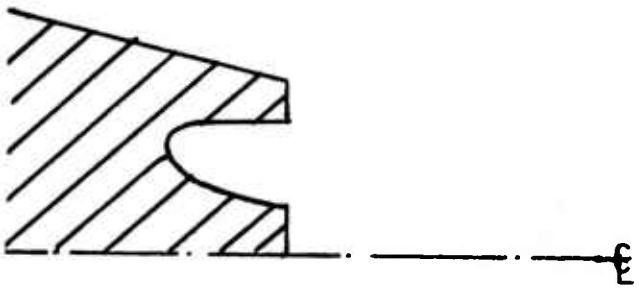

(B)

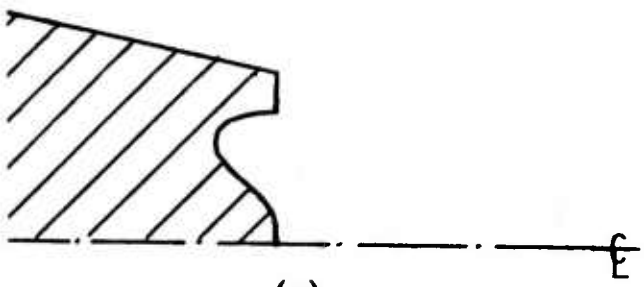

(C)

Figure 4. Base Cavity Configurations of Interest

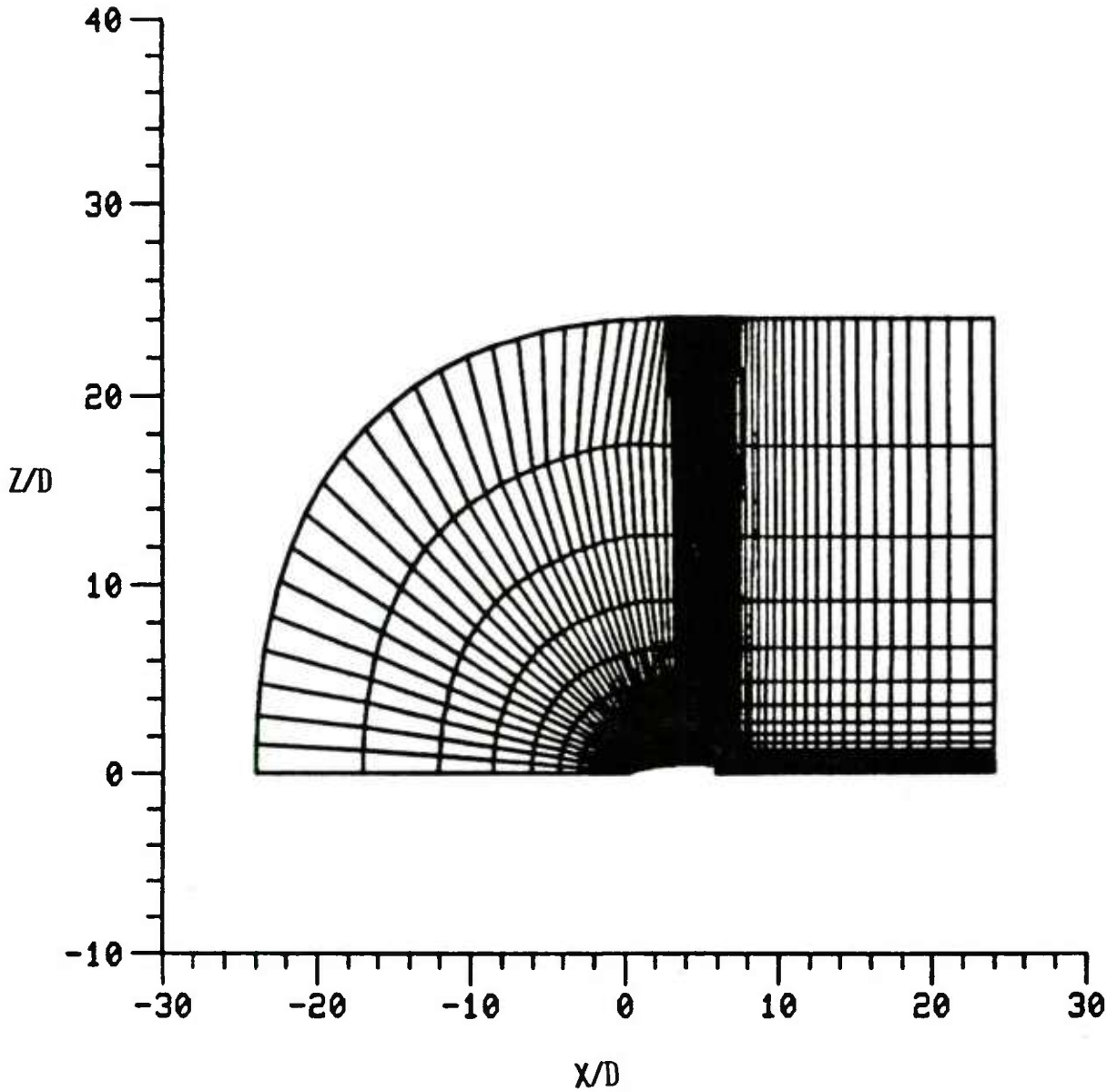

Figure 5. Full Computational Grid

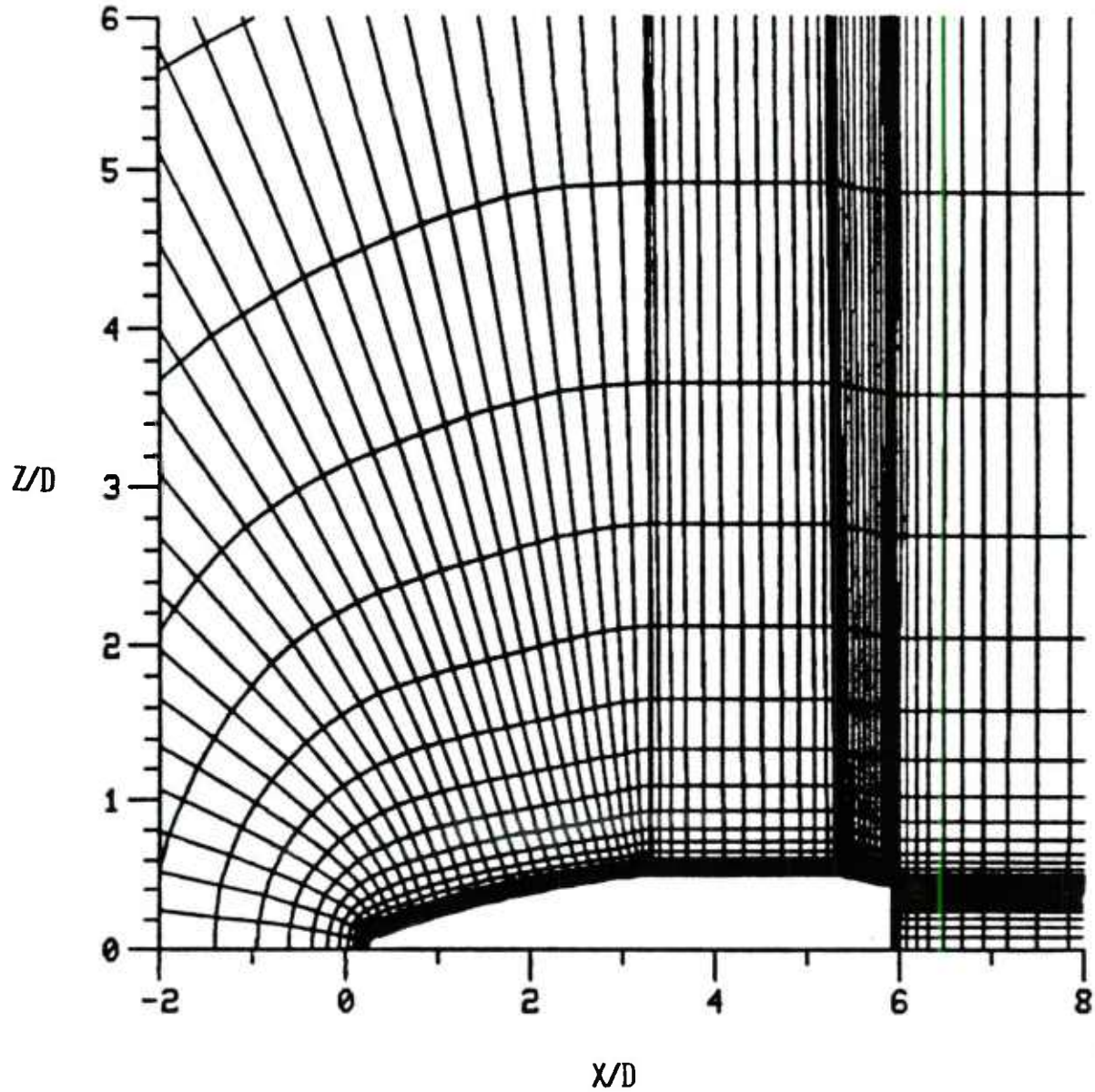

Figure 6. Expanded View of the Grid Near the Model

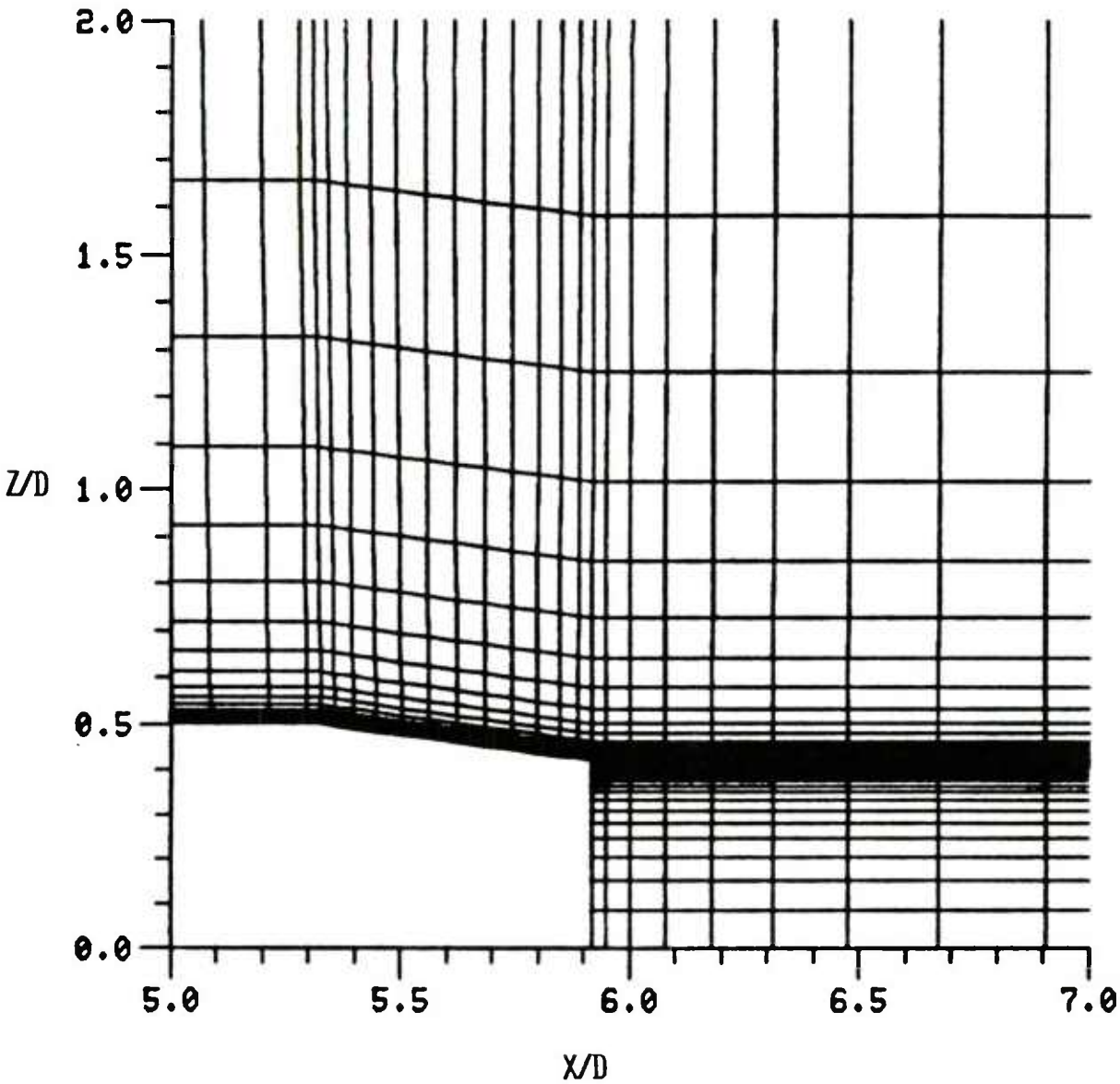

Figure 7. Expanded Grid in the Base Region (without Base Cavity)

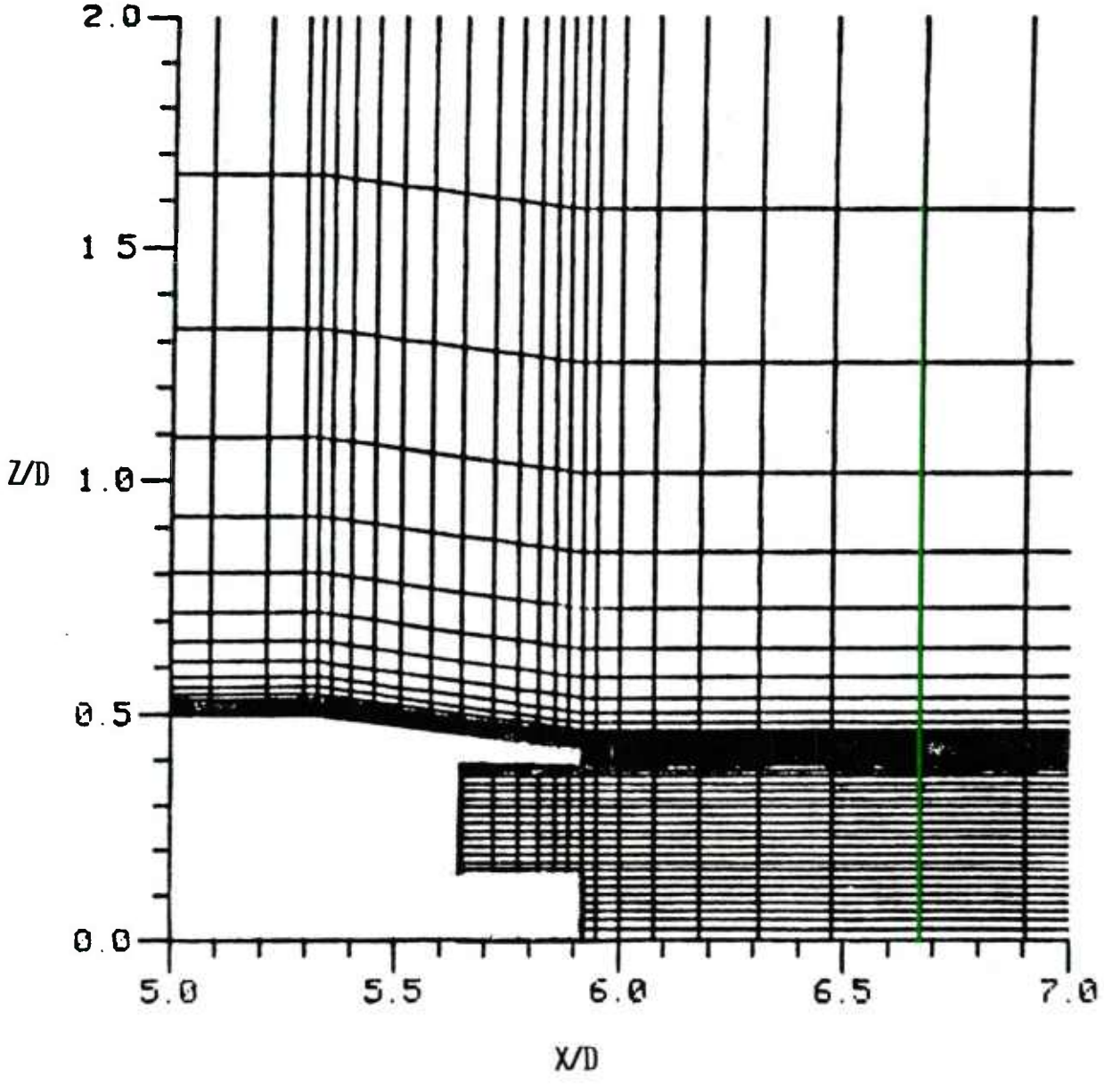

Figure 8. Expanded Grid in the Base Region (with Base Cavity)

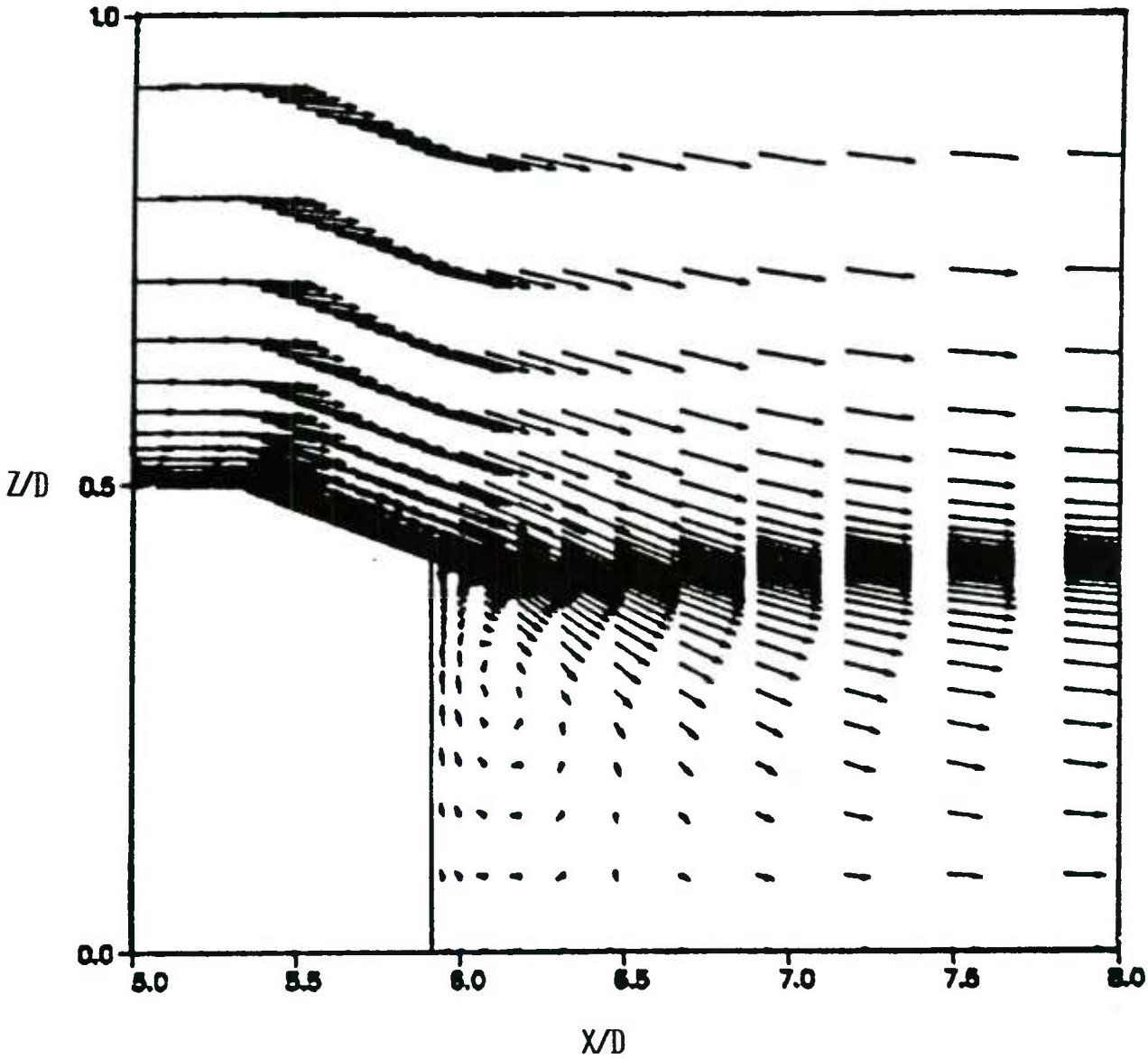

Figure 9. Velocity Vectors, M_∞ = .9, α = 0 (without Base Cavity)

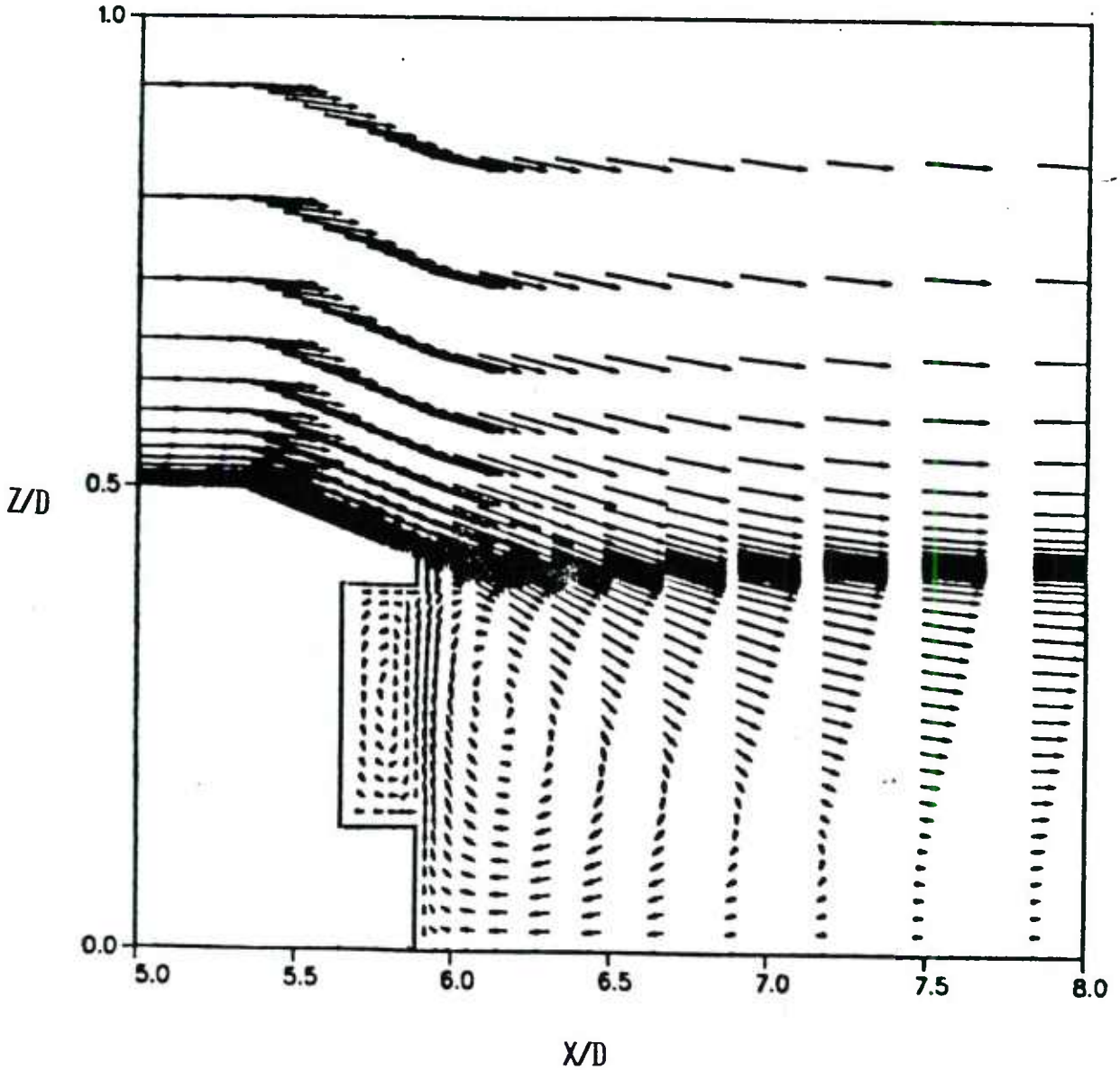

Figure 10. Velocity Vectors, M_∞ = .9, α = 0 (with Base Cavity)

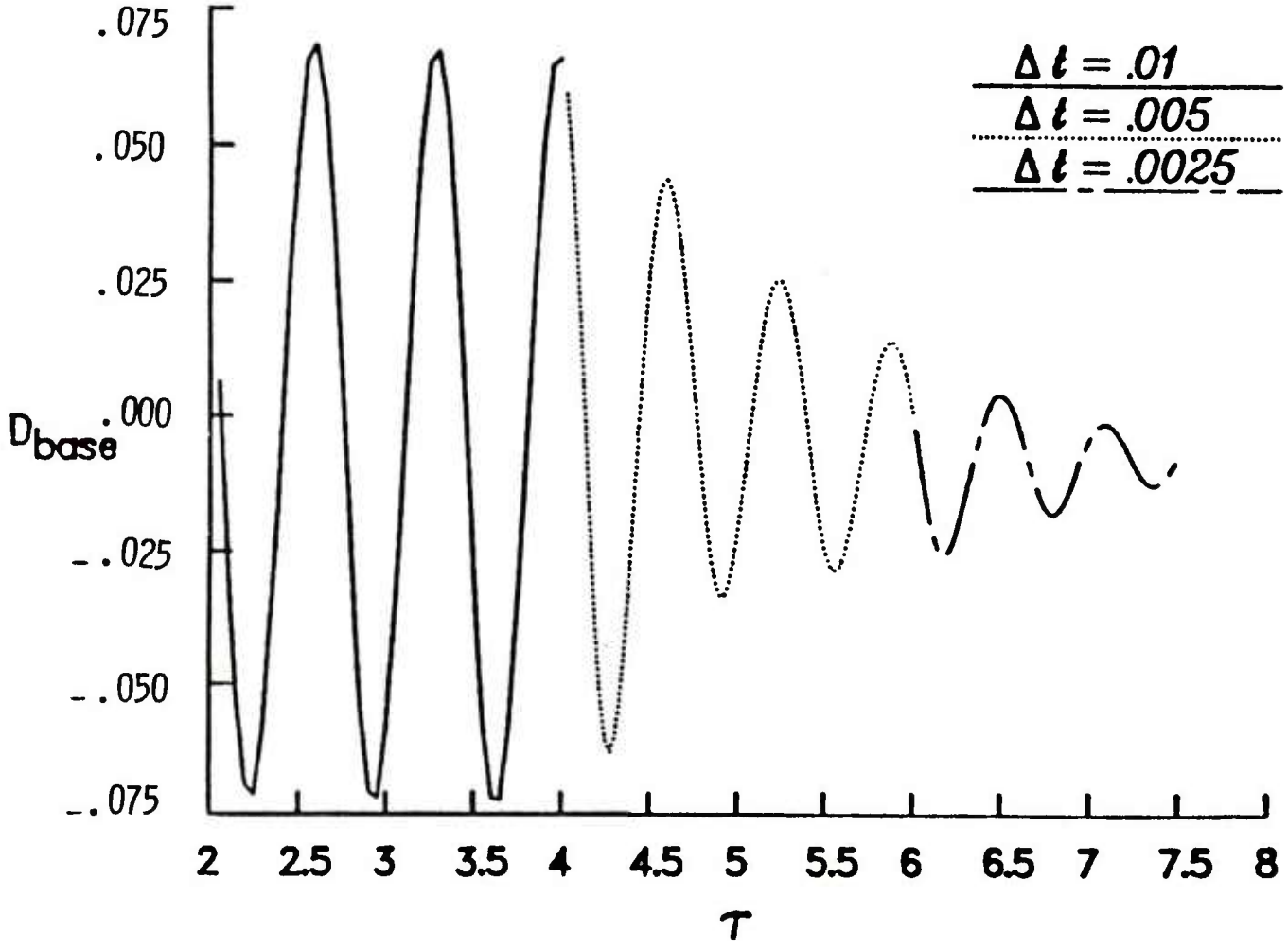

Figure 11. Base Drag vs. Non-dimensional Time

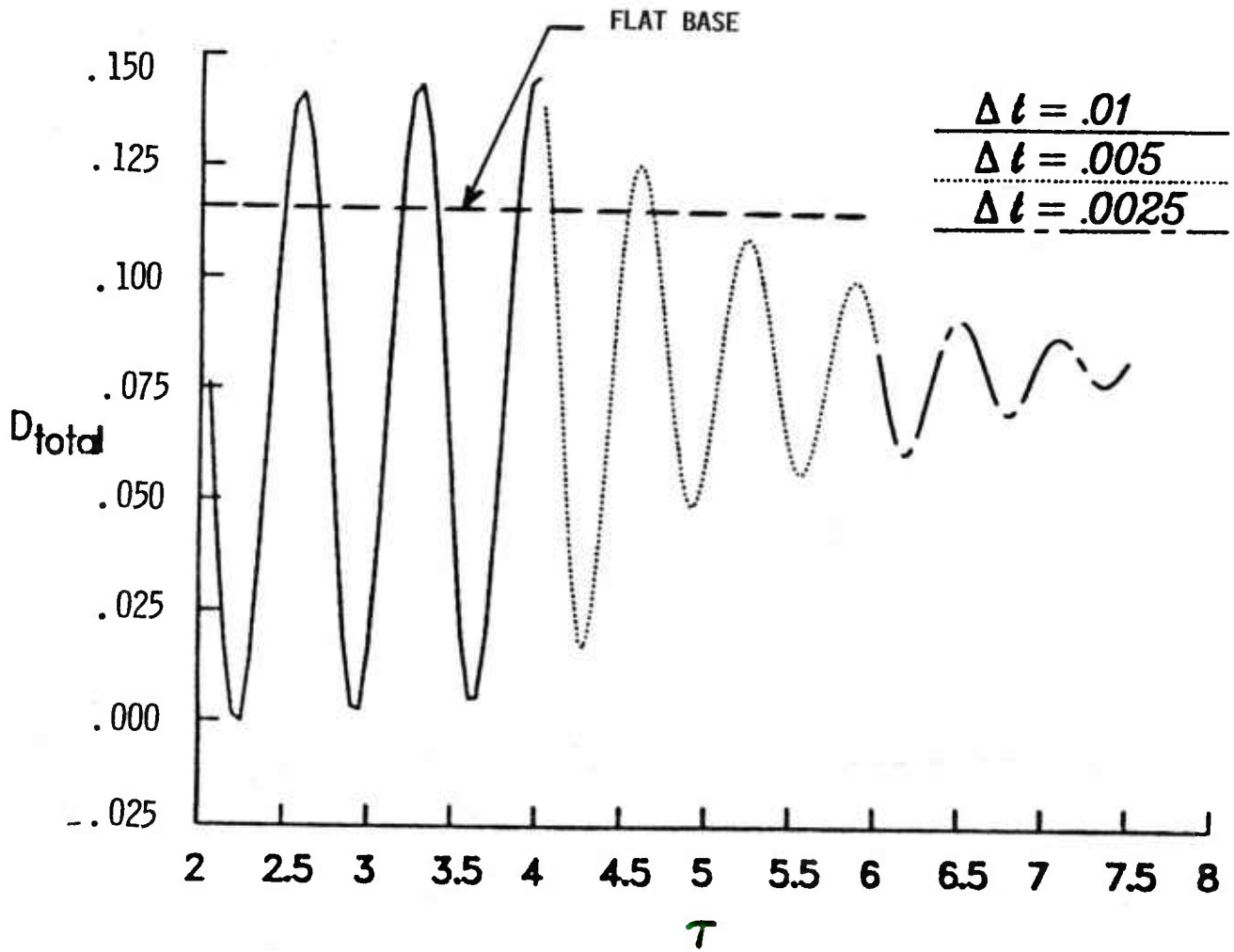

Figure 12. Total Drag vs. Non-dimensional Time

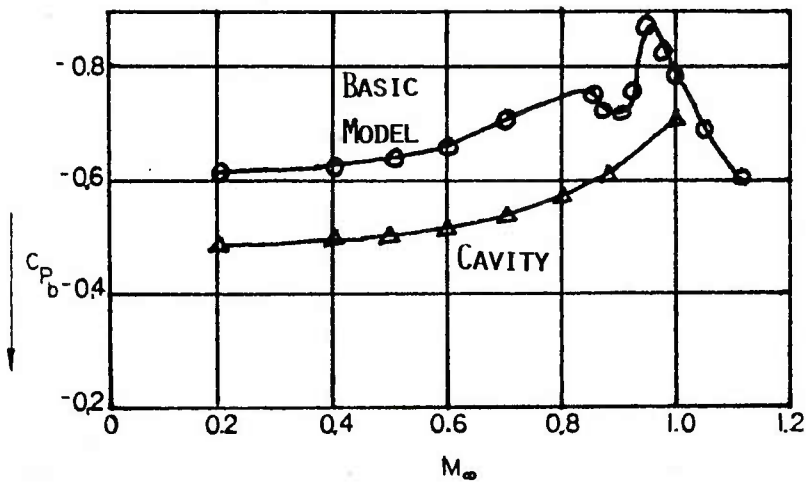

Figure 13. Base Pressure Coefficient vs. Mach Number under Different Base Configurations (Reference 13)

REFERENCES

1. Private Communications with Mr. Richard Eitemiller of the Firing Tables Branch, Launch and Flight Division, BRL, June 1983.

2. C. J. Nietubicz, R. LaFarge, J. Sahu, and D. C. Mylin, "Aerodynamic Coefficient Predictions for a Projectile Configuration at Transonic Speeds," AIAA Paper No. 84-0326, January 1984.

3. C. J. Nietubicz, T. H. Pulliam, and J. L. Steger, "Numerical Solution of the Azimuthal-Invariant Thin-Layer Navier-Stokes Equations," U.S. Army Ballistic Research Laboratory, Aberdeen Proving Ground, Maryland, ARBRL-TR-02227, March 1980. (AD A085716) (Also see AIAA Paper No. 79-0010, January 1979.

4. B. S. Baldwin, and H. Lomax, "Thin-Layer Approximation and Algebraic Model for Separated Turbulent Flows," AIAA Paper No. 78-257, 1978.

5. R. Beam, and R. F. Warming, "An Implicit Factored Scheme for the Compressible Navier-Stokes Equations," AIAA Journal, Vol. 16, No. 4, April 1978, pp. 393-402.

6. J. L. Steger, "Implicit Finite Difference Simulation of Flow About Arbitrary Geometries with Application to Airfoils," AIAA Journal, Vol. 16, No. 4, July 1978, pp. 679-686.

7. T. H. Pulliam, and J. L. Steger, "On Implicit Finite-Difference Simulations of Three-Dimensional Flow," AIAA Journal, Vol. 18, No. 2, February 1980, pp. 159-167.

8. J. Sahu, C. J. Nietubicz, and J. L. Steger, "Numerical Computation of Base Flow for a Projectile at Transonic Speeds," U.S. Army Ballistic Research Laboratory, Aberdeen Proving Ground, Maryland, ARBRL-TR-02495, June 1983. (AD A130293) (Also see AIAA Paper No. 82-1358, August 1982).

9. J. Sahu, C. J. Nietubicz, and J. L. Steger, "Navier-Stokes Computations of Projectile Base Flow with and without Base Injection," U.S. Army Ballistic Research Laboratory, Aberdeen Proving Ground, Maryland, ARBRL-TR-02532, November 1983. (AD A135783) (Also see AIAA Paper No. 83-0224, January 1983).

10. E. D. Boyer, "Free Flight Tests of the SAMOS Re-entry Configuration," U.S. Army Ballistic Research Laboratory, Maryland, ARBRL-MR-1321, February 1961. (AD 374655L)

11. J. L. Steger, C. J. Nietubicz, and K. R. Heavey, "A General Curvilinear Grid Generation Program for Projectile Configurations," U.S. Army Ballistic Research Laboratory, Maryland, ARBRL-MR-03142, October 1981. (AD A107334)

12. D. Degani, and J. L. Steger, "Comparison Between Navier-Stokes and Thin-Layer Computations for Separated Supersonic Flow," AIAA Journal, Vol. 21, No. 11, November 1983, pp. 1604-1606.

13. S. N. B. Murthy (Ed.), "Progress in Astronautics and Aeronautics: Aerodynamics of Base Combustion," Vol. 40, AIAA, New York, 1976, pp. 90-92.

LIST OF SYMBOLS

a	=	speed of sound
a_∞	=	free stream speed of sound
C_p	=	pressure coefficient, $2(p - p_\infty)/\rho_\infty u_\infty^2$
D	=	body diameter (57.15mm)
e	=	total energy per unit volume/$\rho_\infty a_\infty^2$
$\hat{q}$	=	vector of dependent variables
$\hat{E}$, $\hat{F}$	=	flux vector of transformed Navier-Stokes equations
$\hat{H}$	=	n-invariant source vector
J	=	Jacobian of transformation
M	=	Mach number
M_∞	=	free stream Mach number
p	=	pressure/$\rho_\infty a_\infty^2$
p_∞	=	free stream pressure
Pr	=	Prandtl number, $\mu_\infty c_p/\kappa_\infty$
R	=	body radius
Re	=	Reynolds number, $\rho_\infty a_\infty D/\mu_\infty$
$\hat{S}$	=	viscous flux vector
t	=	physical time
u,v,w	=	Cartesian velocity components/a_∞
u_∞	=	free stream velocity
U,V,W	=	Contravariant velocity components/a_∞
x,y,z	=	physical Cartesian coordinates
α	=	angle of attack
γ	=	ratio of specific heats
κ	=	coefficient of thermal conductivity/κ_∞
κ_∞	=	coefficient of thermal conductivity at free stream conditions

μ = coefficient of viscosity/μ_∞

μ_∞ = coefficient of viscosity at free stream conditions

ξ,η,ζ = transformed coordinates in axial, circumferential and radial directions

ρ = density/ρ_∞

ρ_∞ = free stream density

τ = transformed time

ϕ = circumferential angle

Superscript

$*$ = critical value

Subscript

b = base

DISTRIBUTION LIST

No. of Copies	Organization
12	Administrator Defense Technical Info Center ATTN: DTIC-DDA Cameron Station Alexandria, VA 22304-6145
1	HQDA DAMA-ART-M Washington, DC 20310
1	Commander US Army Materiel Command ATTN: AMCDRA-ST 5001 Eisenhower Avenue Alexandria, VA 22333-0001
6	Commander Armament R&D Center US Army AMCCOM ATTN: SMCAR-TDC SMCAR-TSS SMCAR-LCA-F Mr. D. Mertz Mr. A. Loeb Mr. H. Hudgins Mr. E. Friedman Dover, NJ 07801
1	Commander US Army Armament, Munitions and Chemical Command ATTN: SMCAR-ESP-L Rock Island, IL 61299
1	Director Benet Weapons Laboratory Armament R&D Center US Army AMCCOM ATTN: SMCAR-LCB-TL Watervliet, NY 12189
1	Commander US Army Aviation Research and Development Command ATTN: AMSAV-E 4300 Goodfellow Blvd. St. Louis, MO 63120
1	Director US Army Air Mobility Research and Development Laboratory Ames Research Center Moffett Field, CA 94035
1	Commander US Army Communications - Electronics Command ATTN: AMSEL-ED Fort Monmouth, NJ 07703
1	Commander US Army Electronics Research and Development Command Technical Support Activity ATTN: DELSD-L Fort Monmouth, NJ 07703-5301
3	Commander US Army Missile Command ATTN: AMSMI-R AMSMI-RDK Dr. B. Walker Mr. R. Deep Redstone Arsenal, AL 35898
1	Commander US Army Missile Command ATTN: AMSMI-YDL Redstone Arsenal, AL 35898
1	Commander US Army Tank Automotive Command ATTN: AMSTA-TSL Warren, MI 48090
1	Director US Army TRADOC Systems Analysis Activity ATTN: ATAA-SL White Sands Missile Range, NM 88002
1	Commander US Army Research Office P. O. Box 12211 Research Triangle Park, NC 27709-2211

DISTRIBUTION LIST

No. of Copies	Organization
1	Commander US Naval Air Systems Command ATTN: AIR-604 Washington, D. C. 20360
1	Commander US Naval Surface Weapons Center ATTN: Dr. F. Moore Dahlgren, VA 22448
1	Commander US Naval Surface Weapons Center ATTN: Dr. U. Jettmar Silver Spring, MD 20910
1	Commander US Naval Weapons Center Tech Services Br, Code 3433 China Lake, CA 93555
1	Commander US Army Development & Employment Agency ATTN: MODE-TED-SAB Fort Lewis, WA 98433
1	Director NASA Langley Research Center ATTN: NS-185, Tech Lib Langley Station Hampton, VA 23365
4	Director NASA Ames Research Center ATTN: MS-202A-14, Dr. P. Kutler MS-202-1, Dr. T. Pulliam Dr. J. Steger MS-227-8, Dr. L. Schiff Moffett Field, CA 94035
1	Commandant US Army Infantry School ATTN: ATSH-CD-CSO-OR Fort Benning, GA 31905
1	AFWL/SUL Kirtland AFB, NM 87117
1	Air Force Armament Laboratory ATTN: AFATL/DLODL Eglin AFB, FL 32542-5000
2	Director Sandia National Laboratory ATTN: Division No. 1331, Mr. H.R. Vaughn Dr. F. Blottner P.O. Box 580 Albuquerque, NM 87184
1	AEDC Calspan Field Services ATTN: MS 600 (Dr. John Benek) Arnold AFB, TN 37389
1	Virginia Polytechnic Institute & State University ATTN: Dr. Clark H. Lewis Department of Aerospace & Ocean Engineering Blacksburg, VA 24061
1	University of California, Davis Department of Mechanical Engineering ATTN: Prof. H.A. Dwyer Davis, CA 95616
1	University of Delaware Mechanical and Aerospace Engineering Department ATTN: Dr. J. E. Danberg Newark, DE 19711
1	University of Florida Dept. of Engineering Sciences College of Engineering ATTN: Prof. C. C. Hsu Gainesville, FL 32611
1	University of Illinois at Urbana Champaign Department of Mechanical and Industrial Engineering ATTN: Prof. W. L. Chow Urbana, IL 61801
1	University of Maryland Department of Aerospace Engr. ATTN: Dr. J. D. Anderson, Jr. College Park, MD 20740

DISTRIBUTION LIST

No. of Copies	Organization
1	University of Notre Dame Department of Aeronautical and Mechanical Engineering ATTN: Prof. T. J. Mueller Notre Dame, IN 46556
1	University of Texas Department of Aerospace Engineering and Engineering Mechanics ATTN: Dr. D. S. Dolling Austin, Texas 78712-1055
	Aberdeen Proving Ground
	Dir, USAMSAA ATTN: AMXSY-D AMXSY-MP, H. Cohen
	Cdr, USATECOM ATTN: AMSTE-TO-F
	Cdr, CRDC, AMCCOM ATTN: SMCCR-RSP-A SMCCR-MU SMCCR-SPS-IL

USER EVALUATION SHEET/CHANGE OF ADDRESS

This Laboratory undertakes a continuing effort to improve the quality of the reports it publishes. Your comments/answers to the items/questions below will aid us in our efforts.

1. BRL Report Number_____ Date of Report_____

2. Date Report Received_____

3. Does this report satisfy a need? (Comment on purpose, related project, or other area of interest for which the report will be used.)_____

_____

_____

4. How specifically, is the report being used? (Information source, design data, procedure, source of ideas, etc.)_____

_____

_____

5. Has the information in this report led to any quantitative savings as far as man-hours or dollars saved, operating costs avoided or efficiencies achieved, etc? If so, please elaborate._____

_____

_____

6. General Comments. What do you think should be changed to improve future reports? (Indicate changes to organization, technical content, format, etc.)

_____

_____

_____

CURRENT ADDRESS

_____
Name

_____
Organization

_____
Address

_____
City, State, Zip

7. If indicating a Change of Address or Address Correction, please provide the New or Correct Address in Block 6 above and the Old or Incorrect address below.

OLD ADDRESS

_____
Name

_____
Organization

_____
Address

_____
City, State, Zip

(Remove this sheet along the perforation, fold as indicated, staple or tape closed, and mail.)